Determination of Individual Side-Chain Conformations, Tertiary Conformations, and Molecular Topography of Tyrocidine A from Scalar Coupling Constants and Chemical Shifts†

Mei-Chang Kuo and William A. Gibbons*

ABSTRACT: We report for the decapeptide tyrocidine A: (a) H^{α} and H^{β} chemical shifts and scalar coupling constants for most residues of tyrocidine A in methanol-d_4 and dimethyl-d_6 sulfoxide (Me_2SO-d_6) and the H^{α} and H^{β} chemical shifts for other residues; (b) scalar coupling constants $^3J_{\alpha\beta}$ for nine side chains in methanol-d_4 but only seven side chains in Me_2SO-d_6, due to chemical shift degeneracy; the Gln^9 and Tyr^{10} side chains in methanol-d_4 were only approximately analyzed; (c) a total spin–spin analysis of Pro^5 in Me_2SO-d_6 and, partly by comparison, also in methanol-d_4; (d) conversion of $^3J_{\alpha\beta}$ values to side-chain conformations for all residues in methanol-d_4; comparisons, where possible, led to the conclusion that side-chain conformations are similar in methanol-d_4 and Me_2SO-d_6; (e) an absolute conformational analysis of Pro^5 from ^3J values and a method of assigning all *pro-R,S* protons; Pro^5 has a Ramachandran B, C_2–C_{exo}–C_{endo} conformation; (f) χ^1,χ^2 conformations of several aromatic residues based upon proton–chromophore distance measurement from anomalous chemical shifts and Johnson–Bovey diagrams; (g) *pro-R* and *pro-S* assignments of H^{β}'s from anomalous chemical shifts, high-temperature dependence of anomalous chemical shifts, and backbone side-chain nuclear Overhauser effects; (h) most tertiary conformations of the whole tyrocidine A molecule possessing residues 4–8 and 10 in highly preferred (ca. 90%) χ^1 conformations, but residues 1–3 and 9 having at least two χ^1 rotamers; (i) description of three topographical regions of the molecule—a hydrophobic region, a flat hydrophilic surface on the other side of the molecule, and a hydrophilic region consisting of two peptide backbone units and the side chains of Asn^8, Gln^9, and Tyr^{10}; (j) proposed side chain, β-turn, and β-pleated sheet conformations that readily account for all "normal" and anomalous chemical shifts.

Tyrocidine A, a cyclic decapeptide of the tyrothricin family of antibiotics, has the sequence Val^1-Orn^2-Leu^3-D-Phe^4-Pro^5-Phe^6-D-Phe^7-Asn^8-Gln^9-Tyr^{10}; the Val^1...Pro^5 pentapeptide sequence is similar to that of gramicidin S. It has been claimed to be an ionophore, and a cationic detergent, and to effect sporulation in bacteria (Schröder & Lubke, 1966; Lee et al., 1975; Ristow, 1977; Sarkar & Paulus, 1972). The NH–$C^{\alpha}H$ resonances in dimethyl-d_6 sulfoxide (Me_2SO-d_6)[1] were assigned by difference scalar decoupling (DSD)[2] (Gibbons et al., 1975a; Kuo & Gibbons, 1979) and by nuclear Overhauser effect difference spectroscopy (NOEDS) (Gibbons et al., 1975b; Kuo & Gibbons, 1979). A secondary conformation has been proposed (Beyer et al., 1972; Wyssbrod et al., 1973; H. R. Wyssbrod, M. Fein, M. Kuo, and W. A. Gibbons, unpublished experiments).

Here we report on (a) a spin–spin analysis of all $C^{\alpha}H$–$C^{\beta}H_2$ spin systems in methanol-d_4 to yield chemical shifts and scalar coupling constants and the effect of solvent upon these parameters, (b) the χ^1 conformations for side chains from scalar coupling constants, (c) a total spin–spin analysis of proline and a novel approach to unequivocal conformational analysis of prolyl residues and *pro-R,S* assignments, (d) *R* and *S* assignments, proton–chromophore distances, and χ^2 determination from anomalous chemical shifts and correlation of backbone and secondary conformations with normal and anomalous chemical shifts, (e) determination of the major tertiary conformations, and (f) the molecular topography.

Materials and Methods

Samples contained 5 mg of tyrocidine A in 0.4 mL of 99.96% Me_2SO-d_6 or 99.96% methanol-d_4. The tyrocidines were a gift from the late Professor L. C. Craig and had been purified by countercurrent distribution. All the chemical shifts reported refer to the internal standard hexamethyldisilane (HMS). Probe temperatures were measured with a YSI Model 42 SC telethermometer calibrated with methanol and ethylene glycol standard samples (Yellow Springs Instrument Co., Yellow Springs, OH). All ^1H nuclear magnetic resonance (NMR) spectra were taken on a Bruker WH-270 spectrometer (Bruker Instruments, Inc., Billerica, MA) equipped with a 48K-memory Nicolet 1180 computer (Nicolet Instrument Corp., Madison, WI) and operating in the Fourier transform mode. For triple resonance experiments, the decoupler frequency was modulated to produce two side bands. The frequency of modulation was half the difference in chemical shift of the two proton multiplets to be simultaneously decoupled; the decoupler was set halfway between these two frequencies.

Two forms of difference double resonance were used. For DSD spectra, the off-resonance (control) and on-resonance spectra were obtained in the HD mode (the decoupler is on both before and during the observing pulse) of the spectrom-

† From the Department of Biochemistry, College of Agriculture and Life Sciences, University of Wisconsin, Madison, Wisconsin 53706. *Received January 10, 1979; revised manuscript received September 27, 1979.* This work was supported by grants from the National Institutes of Health (AM 18604), the National Science Foundation (BMS 74.23819 and PCM 77.3976), and the College of Agriculture and Life Science of the University of Wisconsin. Partial expenses for the Bruker WH-270 campus facility were provided by the Graduate School Research Committee and University of Wisconsin Biomedical Research Grant No. 07098.

[1] Abbreviations used: Me_2SO-d_6, perdeuterated dimethyl sulfoxide; DSD, difference scalar decoupling; NOEDS, nuclear Overhauser effect difference spectroscopy; NMR, proton magnetic resonance.

[2] Two forms of difference double resonance are used. DSD spectra refer to spectra in which both collapse of scalar multiplets and NOE effects can be observed. Usually, the collapsed multiplets are more obvious than the NOE effects. In NOEDS there is no multiplet collapse; only NOE effects are seen. Strictly speaking, therefore, DSD is a misnomer.

0006-2960/79/0418-5855$01.00/0

Table I: Proton Chemical Shifts[a] of Tyrocidine A in Two Solvents[b]

	NH	H^{α}	H^{β}	H^{γ}	H^{δ}	H^{ϵ}
Val[1]	(7.39_9)	4.77_0 (4.52_1)	2.14_4 (1.96_6)	1.08_1 (0.87_3)		
Orn[2]	(8.85_6)	5.42_0 (5.25_8)	2.0_7 (1.7_2)	1.7_2 (1.6_4)	2.8_9 (2.7_5)	(7.42_2)
			2.1_8 (1.6_4)	1.7_2 (1.6_4)	2.8_2 (2.7_5)	
Leu[3]	(7.88_7)	4.86_0 (4.51_0)	1.6_5 (1.3_3)	1.6_3 (1.4_3)	1.0_2 (0.9_1)	
			1.4_4 (1.2_3)		1.0_0 (0.8_8)	
D-Phe[4]	(9.26_2)	4.42_8 (4.23_3)	3.17_3 (2.91_7)			
			3.10_8 (2.77_2)			
Pro[5]		4.09_6 (4.02_7)	1.4_1 (1.42_0)	1.4_1 (0.9_7)	3.31_7 (3.25_9)	
			1.2_8 (1.10_6)	0.35_2 (0.33_0)	2.15_1 (2.12_5)	
Phe[6]	(7.18_7)	4.50_9 (4.45_0)	2.37_0 (2.20_9)			
			2.21_4 (2.17_0)			
D-Phe[7]	(9.01_3)	5.97_3 (5.54_6)	3.22_2 (2.96_0)			
			2.83_9 (2.68_7)			
Asn[8]	(9.00_7)	4.63_0 (4.46_9)	3.27_2 (3.34_6)		(7.99_4)	
			3.12_8 (3.00_0)		(7.42_2)	
Gln[9]	(8.71_7)	4.00_8 (3.78_0)	1.7_2 (1.6_1)	2.1_0 (1.9_4)		(7.18_1)
			1.7_2 (1.6_1)	2.1_0 (1.9_4)		(6.86_2)
Tyr[10]	(8.40_0)	4.57_3 (4.28_0)	3.04_8 (2.89_7)		6.83_3 (6.88_8)	6.49_1 (6.58_8)

[a] The temperature was 26 °C. [b] The parentheses and the nonparentheses indicated Me_2SO-d_6 and CD_3OD, respectively.

eter, subtracted in the time domain, and transformed to give the difference spectra (Kuo et al., 1979). For NOEDS spectra (Gibbons et al., 1975b) the on- and off-resonance spectra were taken in the HG mode (typically, a 2-s irradiation of a given frequency preceded the observing pulses). In DSD spectra both collapse of scalar multiplets and NOE effects were observed, the collapsed multiplets usually being more obvious than the NOE effects. In NOEDS no multiplet collapse was seen; only changes in intensity of multiplets were seen. Strictly speaking, therefore, DSD is a misnomer.

In all experiments, the spectra were collected in 8K of memory and transformed at 16K or 32K memory, depending on the requirements of digital resolution. The spectral width was 3012 Hz, and before transformation a 1-Hz line broadening was used to enhance the signal to noise ratio. All the reported chemical shifts refer to the internal standard hexamethyldisilane (HMS).

In order to perform non-first-order ABX spin–spin analysis of side chains, we obtained information from three sources—the H^{α} multiplets, the DSD multiplets, and the decoupled spectra themselves. These gave approximate chemical shifts and coupling constants which were used as a starting point for simulation of the DSD spectra. The chemical shifts and coupling constants were varied until a good fit between the observed and simulated DSD spectra resulted. The general procedure for obtaining the approximate δ and J values of the ABX spectrum was as follows. (1) Inspection of the DSD multiplets of the AB parts (β protons) in principle revealed the positions of the eight positive and four negative lines of the nondecoupled and X-decoupled spectra, respectively (Gibbons et al., 1975a). The four negative lines of the AB quartet gave quite accurate values of $^2J_{AB}$, as well as the chemical shifts of β protons and their difference, $\delta_A - \delta_B$. (2) Inspection of the H^{α} multiplet gave $\langle {}^3J_{AX} + {}^3J_{BX} \rangle$ values. The stronger the A and B proton coupling [the smaller the ratio of $(\delta_A - \delta_B)/{}^2J_{AB}$], the less reliable the latter became. (3) When $\delta_A - \delta_B$ was sufficiently large (>30 Hz), irradiation of each A or B proton collapsed the H^{α} multiplets from which approximate $^3J_{AX}$ and $^3J_{BX}$ values were obtained. (4) Simulation of both the H^{α} multiplet and the DSD spectrum of the ABX spin system refined the above parameters.

When residues contained γ and δ protons such as Orn[2], Leu[3], Pro[5], and Gln[9], we obtained H^{α}–H^{β} vicinal coupling constants from the H^{α} quartets directly or H^{α} spectra where each of the β protons was separately decoupled. Whether or not this procedure was valid or feasible was again easily discerned from $\delta_A - \delta_B$ obtained from DSD spectra; i.e., the hidden β proton chemical shifts were revealed (Gibbons et al., 1975a) by this process. When $\delta_A - \delta_B$ was too small and the spin system was degenerate, we reported $\langle {}^3J_{AX} + {}^3J_{BX} \rangle$, e.g., Gln[9].

Often when simulated DSD spectra were compared with experimental DSD spectra, the frequencies agreed but the intensities of the $(ab)_D$ or $(ab)_U$ subspectra[3] disagreed. This was due to NOE effects; in the trans–gauche rotamers the gauche β proton is closer (2.5 Å) to the α proton than the trans β proton (3.1 Å) and, depending upon the populations of α–β rotamers, differential NOEs were observed at β protons. These NOEs in Me_2SO-d_6 were negative and in the range 1–10% but were smaller in CD_3OD. The simulated AB parts of the DSD spectra in Me_2SO-d_6 were adjusted for these negative NOEs.

All spectra were simulated by using the ITRCAL program supplied with the Nicolet 1180 computer. The line width at half-height used for the simulated spectra was 3.5 and 4.5 Hz in CD_3OD and Me_2SO-d_6, respectively.

In CD_3OD all H^{α} multiplets were isolated from each other, and few problems were encountered with spin–spin analysis in this solvent. In Me_2SO-d_6, however, Val[1], Leu[3], Asn[8], and Phe[6] overlapped with each other and Phe[4] and Tyr[10] also overlapped. When H^{α} multiplets were obscured by overlap, two methods were used to obtain the individual H^{α} spectra: (a) higher temperature and/or (b) NOEs at α protons resulting from β- or amide-proton (in a partially exchanged sample) irradiation (Kuo & Gibbons, 1979).

Results and Discussion

The chemical shifts of each proton of the NH–$C^{\alpha}H$–$C^{\beta}H_2$ moieties of tyrocidine A in Me_2SO-d_6 have been evaluated by a combination of DSD and NOEDS (Kuo & Gibbons, 1979). Here we will focus upon the determination of the individual side-chain conformations and the tertiary conformations of the whole molecule from H^{α}–H^{β} scalar coupling constants and the correlation of conformation with chemical shifts. A similar study of gramicidin S, a member of the tyrothricin group of peptide antibiotics, has appeared (Jones et al., 1977, 1978a, 1979; Kuo et al., 1979).

[3] βD and βU, γD and γU, etc. refer to the downfield and upfield resonances of the β and γ protons, respectively.

Table II: Side-Chain Scalar Coupling Constants

		$^3J_{\alpha\beta}$ (Hz)							
		CD_3OD			Me_2SO-d_6	$^2J_{\beta\beta}$(26 °C) (Hz)		$\Sigma^3J_{\alpha\beta}$(26 °C) (Hz)	
		26 °C	46 °C	66 °C	26 °C	CD_3OD	Me_2SO-d_6	CD_3OD	Me_2SO-d_6
Val[1]			8.5 ± 0.2	8.3 ± 0.2	7.2 ± 0.2				
Orn[2]	βD	6.0 ± 0.5	6.4 ± 0.5	6.7 ± 0.5					12.5 ± 0.5
	βU	8.5 ± 0.5	8.0 ± 0.5	8.0 ± 0.5					
Leu[3]	βD		8.4 ± 0.5	8.5 ± 0.5					15.0 ± 0.5
	βU		6.0 ± 0.5	5.8 ± 0.5					
D-Phe[4]	βD	4.8 ± 0.5	4.8 ± 0.5	4.9 ± 0.5	5.2 ± 0.2	−12.1 ± 0.5	−12.5 ± 0.5		15.8 ± 0.5
	βU	11.2 ± 0.5	10.7 ± 0.5	10.5 ± 0.5	10.6 ± 0.2				
Pro[5]	βD	1.4 ± 0.5			1.4 ± 0.5				
	βU	7.8 ± 0.2			7.8 ± 0.2				
Phe[6]	βD	12.3 ± 0.2	12.1 ± 0.2	12.0 ± 0.2	3.2 ± 0.2	−13.6 ± 0.2	−13.6 ± 0.2		
	βU	3.5 ± 0.2	3.7 ± 0.2	4.3 ± 0.2	12.6 ± 0.2				
D-Phe[7]	βD	3.1 ± 0.2	3.4 ± 0.2	3.7 ± 0.2	3.5 ± 0.2	−13.6 ± 0.2	−13.6 ± 0.2		
	βU	12.0 ± 0.2	11.7 ± 0.2	11.8 ± 0.2	12.0 ± 0.2				
Asn[8]	βD	2.6 ± 0.2	2.6 ± 0.2	2.6 ± 0.2	2.6 ± 0.2	−16.9 ± 0.2	−16.9 ± 0.2		
	βU	4.4 ± 0.2	4.4 ± 0.2	4.4 ± 0.2	4.0 ± 0.2				
Gln[9]								11.5 ± 0.5	12.5 ± 0.5
Tyr[10]	βD	3.3 ± 0.2	3.5 ± 0.2	3.5 ± 0.2		−13.6 ± 0.2			15.4 ± 0.5
	βU	12.8 ± 0.2	12.6 ± 0.2	12.5 ± 0.2					

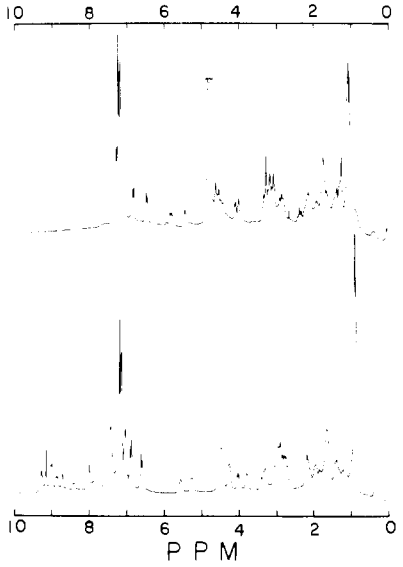

FIGURE 1: The 270-MHz NMR spectrum of tyrocidine A in CD_3OD (top) and Me_2SO-d_6 (bottom). Temperature = 26 °C and concentration = 5 mg/0.4 mL.

Assignments and Spin–Spin Analysis in CD_3OD. The 270-MHz proton NMR spectra of tyrocidine A in CD_3OD and Me_2SO-d_6 are shown in Figure 1; the chemical shift assignments and scalar coupling constants are in Tables I and II, respectively. NMR parameters of the NH–C$^\alpha$H moieties in methanol were obtained by the following: (a) assignments in Me_2SO-d_6 (Kuo & Gibbons, 1979); (b) DSD in CD_3OD; (c) titration from Me_2SO-d_6 into CH_3OH (Fein, 1977; Kuo, 1979) and following the amide-proton chemical shifts.

DSD of tyrocidine A was first attempted by Gibbons et al. (1975a), but our recent NOEDS results showed that these assignments were partially in error (Kuo & Gibbons, 1979). This was not surprising since in Me_2SO-d_6 four H$^\alpha$ multiplets overlap and tyrocidine A possesses five residues (Phe[4], Phe[6], Phe[7], Asn[8], and Tyr[10]) whose H$^\beta$ multiplets can overlap.

All H$^\alpha$ multiplets were resolved in the CD_3OD spectrum (Figure 2), and DSD on each H$^\alpha$ multiplet therefore gave excellent difference spectra (Figure 3A). The spectra were analyzed for all chemical shifts and C$^\alpha$H–C$^\beta$H scalar coupling constants (Tables I and II). When necessary, β protons were irradiated in complementary DSD experiments and concomitant collapse of α and γ protons was observed. It was heartening that the difference spectroscopy assignments in CD_3OD confirmed those achieved by solvent titration and difference spectroscopy in Me_2SO-d_6 (Figure 3B) (Kuo & Gibbons, 1979; Fein, 1977; Kuo, 1979).

Computer simulation of DSD H$^\beta$ multiplets of the ABX residues was performed and compared with authentic spectra. Examples of Phe[6] and Asn[8] are shown in parts A and B of Figure 4.

Analysis was also achieved by simulating the H$^\alpha$ multiplet spectra when each β proton was decoupled (Figure 4). In residues that contained γ protons, no simple eight line/four line difference spectrum was observed, characteristic of ABX multiplets of the four aromatic and Asn[8] residues. Fortunately, however, the βD and βU[3] protons of Orn[2], Leu[3], and Pro[5] were sufficiently resolved (>30 Hz) to decouple each β proton selectively. Extensive decoupling of γ- and δ-proton multiplets confirmed the chemical shift assignments of the β and γ protons, respectively, of these multiplets and helped the analysis of their C$^\alpha$H-C$^\beta$H multiplets. The β protons of Gln[9] were degenerate, and only the sum $^3J_{\alpha\beta D} + {}^3J_{\alpha\beta U}$ was evaluated from its α-proton multiplets.

An analysis of the H$^\gamma$ and H$^\delta$ multiplets of the side chains of Orn[2], Leu[3], and Gln[9] must await extensive synthetic or biosynthetic experiments like those performed for gramicidin S (Jones et al., 1977, 1978a, 1979; Kuo et al., 1979). For the Pro[5] residue, correct values for the chemical shifts of each α, β, γ, and δ proton and vicinal coupling constants for H$^\alpha$–H$^{\beta D}$, H$^\alpha$–H$^{\beta U}$, H$^{\beta U}$–H$^{\gamma U}$, H$^{\gamma U}$–H$^{\delta D}$, and H$^{\gamma D}$–H$^{\gamma U}$ were obtained from decoupling experiments. Since the H$^{\beta D}$ and H$^{\gamma D}$ proton resonances overlapped, fewer ^3J values for Pro[5] were obtained in CD_3OD than in Me_2SO-d_6. Correlations between the chemical shifts in these two solvents were excellent, except for a slight shift of H$^{\gamma D}$ to overlap with H$^{\beta D}$ (see next paragraph).

Assignments and Spin–Spin Analysis in Me_2SO-d_6. The analysis of the H$^\alpha$ and H$^\beta$ multiplets in Me_2SO-d_6 was less complete than that in CD_3OD except for Pro[5] because of spectral overlap and chemical shift degeneracy of certain βD- and βU-proton multiplets. Additional complications and difficulties existed because of overlap of the α-proton multiplets of Val[1], Leu[3], Phe[6], and Asn[8] at ~4.5 ppm and of D-Phe[4] and Tyr[10] at ~4.2 ppm and the degenerate chemical shifts of the β protons of Orn[2], Gln[9], and Tyr[10]. Of the aromatic residues, only the ABX system of D-Phe[7] could be analyzed by simple

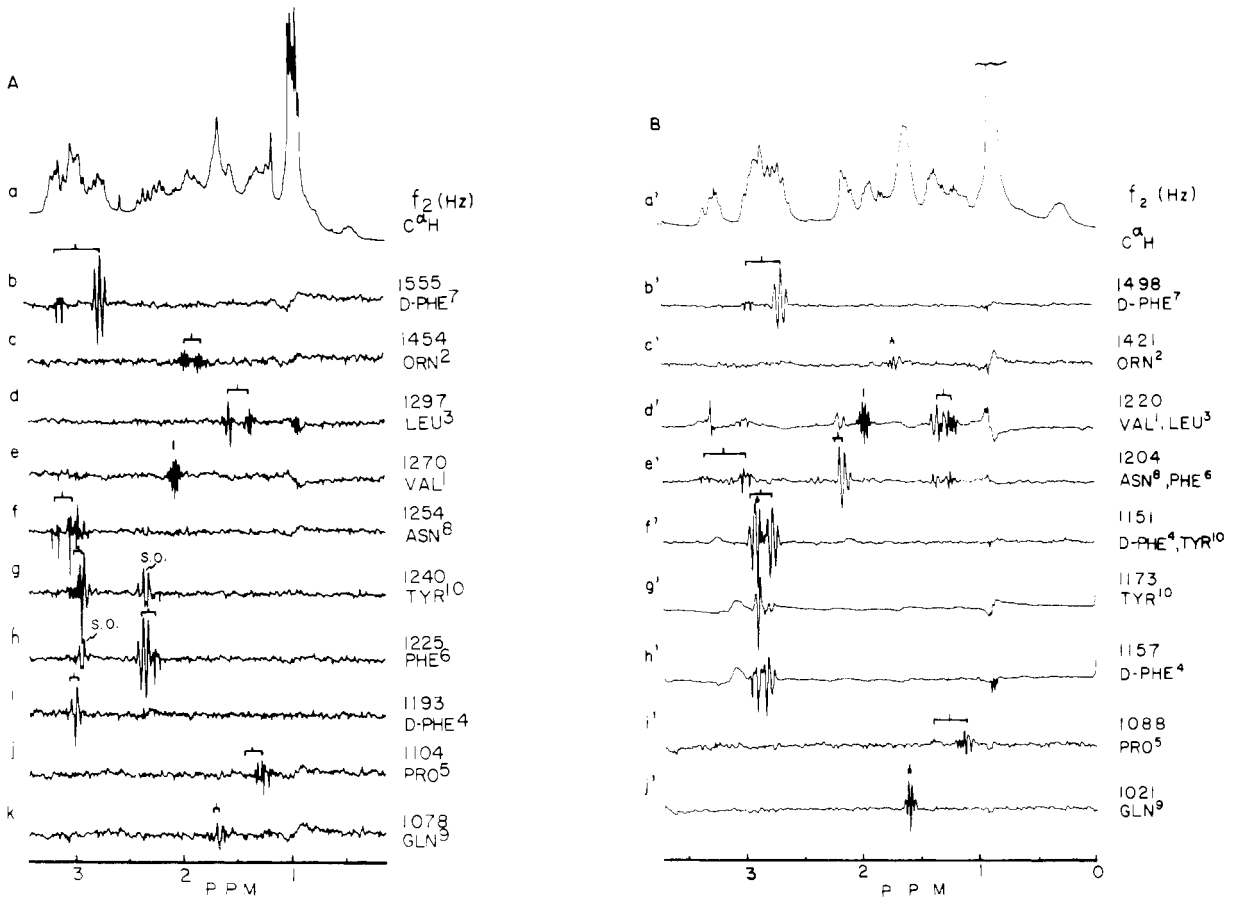

FIGURE 2: Difference double-resonance spectra of tyrocidine A in CD_3OD (A) and Me_2SO-d_6 (B) at 66 and 26 °C, respectively. Concentrations were 5 mg/0.4 mL for both. At the right of each is the frequency in hertz and the identity of the α proton which is decoupled. (b, b'), (c, c'), etc. were obtained by subtracting the decoupled spectrum from the spectrum in which the decoupling frequency was offset, usually by 100 Hz. This minimized Bloch–Siegert effects. (1) α, βD, and βU proton chemical shifts measured from these spectra are in Table I. (2) Many βD and βU multiplets are well separated [e.g., D-Phe^7 in (b) and (b') or Asn^8 in (f) and (e')]. (3) Degenerate or near-degenerate protons are seen in (j') and (k) (Gln^9) and in (g') (Tyr^{10} in Me_2SO-d_6). (4) Decoupler spillover effects (SO) can be seen in (f) (Tyr^{10}H$^\alpha$), (g) (Phe^{6}H$^\alpha$ and Asn^{8}H$^\alpha$), (h) (Tyr^{10}H$^\alpha$), (d') (Asn^{8}H$^\alpha$ and Phe^{6}H$^\alpha$), and (e') (Val^{1}H$^\alpha$ and Leu^{3}H$^\alpha$). (5) (f') demonstrates that the H$^\alpha$ multiplets of D-Phe^4 and Tyr^{10} overlap. The difference spectrum (f') also shows overlap of the four β protons of these residues. (6) (g') and (h') were taken at 86 °C, where the H$^\alpha$ multiplets of D-Phe^4 and Tyr^{10} are partially separated (14 Hz). (7) The βD proton of Pro^5 is difficult to see in (j) and (i') because $^3J_{\alpha\beta}$ = 1.4 Hz. Its existence was demonstrated by irradiation at the frequencies of βD and βU and observation of the collapse of the Pro^{5}H$^\alpha$ multiplet and by decoupling of H$^{\gamma U}$ at ~0.3 ppm. (8) The predominant observable event in these spectra is collapse of scalar coupled multiplets.

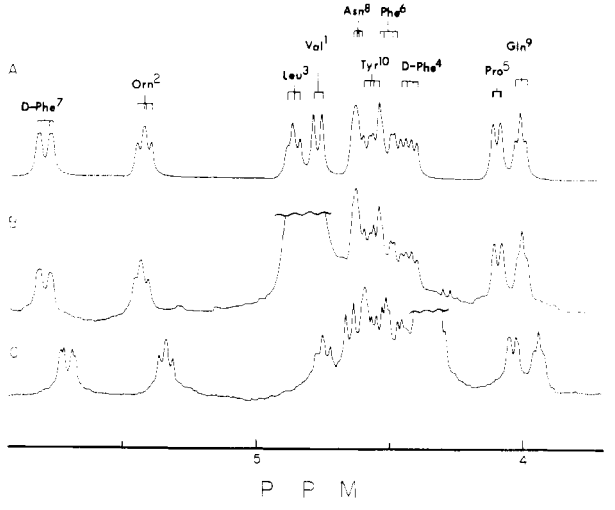

FIGURE 3: (A) The simulated α-proton region of tyrocidine A in CD_3OD at 26 °C. (B) The observed α-proton region of tyrocidine A in CD_3OD at 26 °C. (C) The observed α-proton region of tyrocidine A in CD_3OD at 66 °C. The HDO resonance obscured two H$^\alpha$ multiplets at 26 °C. The $^3J_{\alpha\beta}$ values for these two residues were therefore measured at 46 °C where HDO overlap was absent and used unchanged in the simulations of Figure 3A.

comparison of simulated and observed DSD spectra; other ABX systems required temperature perturbation and/or NOEDS for analysis.

At higher temperatures the H$^\alpha$ multiplets of D-Phe^4 and Tyr^{10} were partially resolved, permitting analysis of the C$^\alpha$H–C$^\beta$H$_2$ spin system of D-Phe^4; Tyr^{10}, however, still possessed a degenerate ABX spin system.

To obtain an analysis of the ABX spin system of Asn^8 whose H$^\alpha$ multiplet overlapped with that of Phe^6, we had to use a combination of DSD and NOEDS. Thus, irradiation of the NH protons of Gln^9 yielded significant NOEs at the βD and βU protons of Asn^8 and Gln^9, permitting complete ABX analysis of Asn^8 (Figure 5); Gln^9 contained a degenerate ABX spin system.

Irradiation of the D-Phe^{4}NH and D-Phe^{4}H$^\alpha$ multiplets gave NOEs at the D-Phe^{4}H$^\beta$ signals. The H$^\beta$ assignments of Tyr^{10} were similarly confirmed by NOE signals obtained by irradiation of its NH and H$^\alpha$ multiplets (Kuo & Gibbons, 1979).

The H$^\alpha$ multiplets of Val^1 and Leu^3 were confirmed and analyzed by preparing a sample of tyrocidine A in which slowly exchanging NH protons were replaced by deuterons (Val^{1}ND, Leu^{3}ND, Asn^{8}ND, and Phe^{6}ND); the other amide doublets were principally in the NH form. Irradiation of Orn^{2}NH,

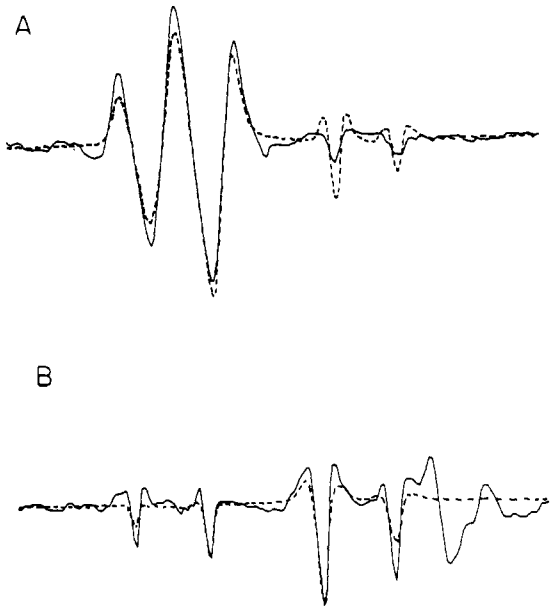

FIGURE 4: NOEDS of Phe[6] (A) and Asn[8] (B) in CD_3OD. In each case the α-proton multiplet was saturated to give the observed (—) spectrum. The corresponding computer-simulated spectra (---) are shown for comparison. (The corresponding H^{α} simulations for these residues are shown in Figure 2A.)

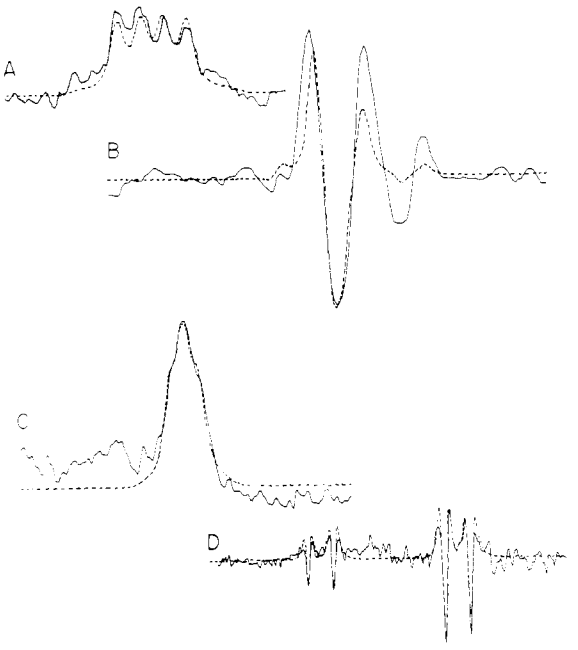

FIGURE 5: (A) and (C) are the simulated (---) and observed (—) α-proton multiplets of the Phe[6] and Asn[8] residues of tyrocidine A in Me_2SO-d_6 at 26 °C. In this case the amide protons of Phe[6] and Asn[8] were fully exchanged for deuterons, and the spectra were obtained by difference NOE experiments by irradiating D-Phe[7]NH and Gln[9]NH, respectively. (B) and (D) are the simulated (---) and observed (—) DSD spectra of the Phe[6] and Asn[8] AB multiplets, respectively.

D-Phe[4]NH, D-Phe[7]NH, and Gln[9]NH yielded NOEs (Kuo & Gibbons, 1979) at the α protons of Val[1], Leu[3], Phe[6], and Asn[8], respectively, which were analyzed for $^3J_{\alpha\beta}$ values (Figure 5).

The seven-spin system of Pro[5] in Me_2SO-d_6 was approximately first order. Because the H^{α}, $H^{\gamma U}$, and $H^{\delta D}$ resonances did not overlap with others in tyrocidine A, triple resonance of the $H^{\beta U}$ and $H^{\delta U}$ multiplets gave analyzable decoupled multiplets at H^{α}, $H^{\gamma U}$, and $H^{\delta D}$. Similar triple resonance experiments plus DSD gave estimates of all Pro[5] coupling

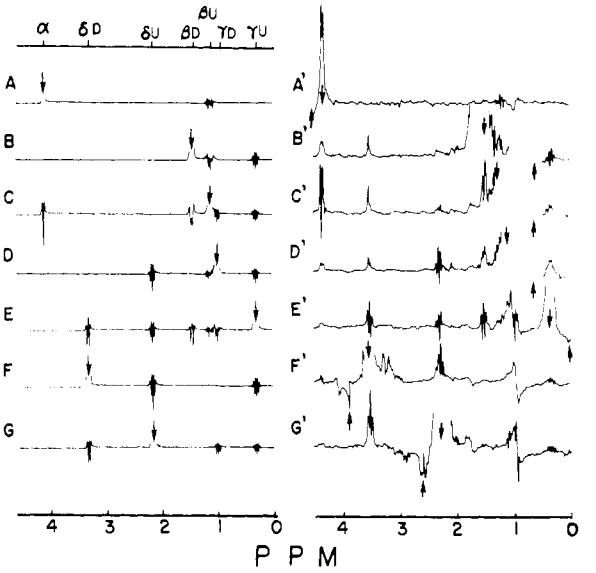

FIGURE 6: DSD spectra of the Pro[5] residue of tyrocidine A in Me_2SO-d_6. The arrows indicate the positions of the decoupling field, f_2 (↓), and the off-resonance decoupling field (↑). (A, A'), (B, B'), (C, C'), etc. are the corresponding simulated and observed DSD spectra of the α, βD, βU, γD, γU, δD, and δU protons, respectively. Differential NOE effects are observable on the scalar multiplets. Irradiation of $H^{\delta U}$ (G') produced a large NOE at $H^{\delta D}$ and a smaller NOE at $H^{\delta U}$ (G'). These NOE effects are not accounted for in (A–G). Irradiation of $H^{\gamma D}$ (D') produced differential NOEs at $H^{\gamma U}$, $H^{\beta D}$, $H^{\delta D}$, and $H^{\delta U}$. Decoupler spillover effects are seen in these spectra.

constants. The constants were used to simulate the spectra in Figure 6A and obtain a total spin–spin analysis in this solvent by comparison with Figure 6B. Thus, the Pro[5] residue was completely analyzed in Me_2SO-d_6 (see later) and partially analyzed in CD_3OD. Where ^3J values were available, they agreed substantially; the $H^{\gamma U}$ and $H^{\delta U}$ chemical shifts anomalous in Me_2SO-d_6 were equally anomalous in CD_3OD.

Thus, six out of ten $C^{\alpha}H$–$C^{\beta}H_2$ multiplets were analyzed in Me_2SO-d_6. The $^3J_{\alpha\beta}$ values for these residues were close to the same values in CD_3OD. The sum, $^3J_{\alpha\beta D} + {}^3J_{\alpha\beta U}$, was evaluated for Leu[3], Gln[9], and Tyr[10]; again, agreement with the corresponding sum in CD_3OD was satisfactory. In the case of Orn[2] the sum $^3J_{\alpha\beta D} + {}^3J_{\alpha\beta U}$ differed by 2.0 Hz between solvents.

Individual Side-Chain Conformations in CD_3OD. The conventional assumptions of rotamer analysis (Pachler, 1964) and the scalar coupling constants, $^3J_{\alpha\beta}$, of Table II were used to calculate the χ^1 rotamers for each amino acid side chain of tyrocidine A in CD_3OD (Figure 7). Use of Pachler's (1964) intrinsic scalar coupling constants led to the conclusion that the D-Phe[4], Phe[6], D-Phe[7], Asn[8], and Tyr[10] side chains had either of two conformational possibilities: (a) classical rotamers with one of the χ^1 rotamers predominantly populated and the others populated according to the Table III data or (b) the side chain frozen in one conformation in which χ^1 deviates slightly (±10°) from the classical χ^1 rotamer angles.

A related interpretation using alternative intrinsic coupling constants (Kopple et al., 1973) was made; namely, within experimental error, one 100% populated classical rotamer exists. Because of the experimental errors in the values of $^3J_{\alpha\beta D}$ and $^3J_{\alpha\beta U}$ and the two Karplus relationships, the conclusions based upon either Kopple's or Pachler's values were essentially the same.

Certain features of the Table III data are quite striking. (a) D-Phe[4], Phe[6], D-Phe[7], Asn[8], and Tyr[10] exist in one predominant rotamer (>78% populated). (b) The Val[1] and Leu[3] residues differ from residues 4, 6–8, and 10 in that they have at least

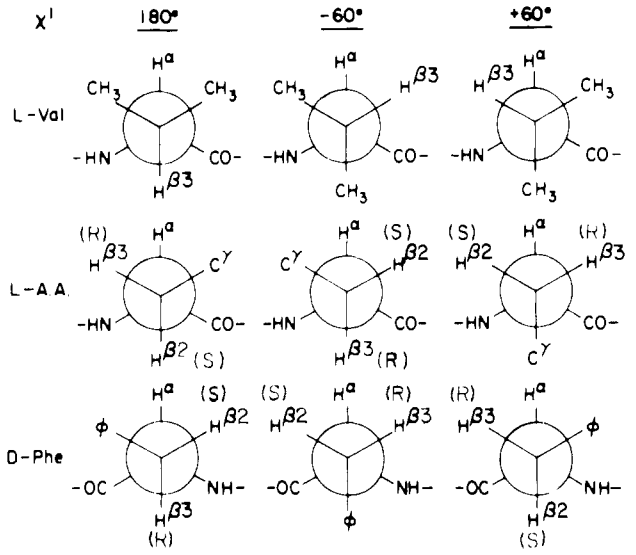

FIGURE 7: The χ^1 rotamers of L-Val, D-Phe, and general L amino acids with two β protons. *R* and *S* β protons are designated in the diagram; in the case of Cys, Asp, and Asn, the *R* and *S* positions are interchanged due to the heavy γ atoms.

Table III: Rotamer Population for χ^1 Rotation in Two Solvents[a]

	180°		−60°		+60°
Val[1]	0.54			0.48[b]	
	(0.42)			(0.58[b])	
Orn[2]	0.31[c]		0.54[c]		0.15
		(0.67[b])			(0.33)
Leu[3]	0.31[c]		0.53[c]		0.15
		(0.89[b])			(0.11)
D-Phe[4]	0.78		0.02		0.20
	(0.73)		(0.03)		(0.24)
Phe[6]	0.10		0.89		0.01
	(0.05)		(0.91)		(0.04)
D-Phe[7]	0.05		0.10		0.86
	(0.08)		(0.06)		(0.86)
Asn[8]	0.16		0.00		0.84
	(0.13)		(0.00)		(0.87)
Gln[9]		0.58[b]			0.42
		(0.67[b])			(0.33)
Tyr[10]	0.07[c]		0.93[c]		0.00
		(0.93[b])			(0.07)

[a] The temperature was 26 °C; parentheses and nonparentheses indicate in Me_2SO-d_6 and CD_3OD, respectively. The Val[1] and Leu[3] populations in CD_3OD are for 46 °C. [b] Sum of two rotamers. [c] Because the *R* and *S* protons are not assigned for these residues, assignment of a population to one or the other of the trans-gauche rotamers was not possible.

two predominant χ^1 rotamers. The crystal structure of L-Leu and derivatives (Lakshminarayanan et al., 1967) having extended backbone structures have $\chi^1,\chi^2 = +60°,+180°$ has not been found in crystals. Our data for Leu in tyrocidine A support the existence of the $\chi^1 = 180°$ and $\chi^1 = -60°$. Presumably, therefore, it is safe to hypothesize the χ^1,χ^2 combinations found theoretically and crystallographically are also those in tyrocidine A (and gramicidin S). Exact comparison of the NMR data with crystal and energy minimization data for Val[1] is premature because the former method has not yet distinguished individual populations for $\chi^1 = +60°$ and $\chi^1 = -60°$ romaters. The sum of these was found to be 47% and the predominant rotamer was $\chi^1 = 180°$. (c) In the sequence 6–10 the Gln[9] residue, which has $^3J_{\alpha\beta D} + {}^3J_{\alpha\beta U} = 11.5$ Hz, differs from residues 6–8 and 10 in that at least two χ^1 rotamers, not one, are significantly populated. At this moment we have no explanation why the conformational state of the side chain of Gln[9] apparently differs significantly from that of D-Phe[4], Pro[5], Phe[6], D-Phe[7], Asn[8], and Tyr[10].

Comparison of these data with the corresponding data for gramicidin S (Jones et al., 1977, 1978a, 1979; Kuo et al., 1979; Rae & Scheraga, 1978), another member of the tyrothricin antibiotic family, is interesting; both molecules contain the sequence Val[1], Orn[2], Leu[3], and D-Phe[4]; except for Orn[2] the most stable rotamer for each residue is more populated for tyrocidine A. The Orn[2] exception is readily explained by the fact that it is the only side chain on one side of the polypeptide backbone, whereas in gramicidin S the two ornithine side chains exhibit Coulombic repulsion.

Individual Side-Chain Conformations in Me_2SO-d_6. Successful rotamer analysis of Val[1], D-Phe[4], Pro[5], Phe[6], D-Phe[7], and Asn[8] was performed; the results in Table III agree substantially with the corresponding methanol data in the same table. The side-chain conformations at the χ^1 level of these residues are therefore substantially independent of solvent. Only $^3J_{\alpha\beta D} + {}^3J_{\alpha\beta U}$ is available for Leu[3], Gln[9], and Tyr[10], but these values are consistent with the essential similarity of χ^1 rotamer populations in CD_3OD.

The values of $^3J_{\alpha\beta D} + {}^3J_{\alpha\beta U}$ for Orn[2] suggest more averaging of χ^1 rotamers in Me_2SO-d_6. It should be noted that all residues are slightly more averaged in Me_2SO-d_6.

Conformational Analysis and Pro-R and Pro-S Assignments of the Prolyl Residue from Spin–Spin Analysis. The Double-Karplus/Ring-Closure Approach. In general, prolyl residue spin–spin analysis in complex peptides has not been rigorously achieved because, in all cases, either the two γ or two β protons have degenerate chemical shifts and, even when all ^3J values were reported, it was not shown which protons of the prolyl ring possessed *pro-R* or *pro-S* configurations. We report here a complete spin–spin analysis of the prolyl residue in tyrocidine A using double- and triple-resonance and DSD spectroscopy. In Me_2SO-d_6 this residue approximates a first-order coupled seven-spin system; in CD_3OD only a partial analysis could be achieved by these methods, but, due to the remarkably close agreement between all available NMR parameters in CD_3OD and DMSO-d_6, especially highly anomalous chemical shifts and $^3J_{\alpha\beta}$ values, it is not unreasonable to propose that the tyrocidine A prolyl residue has the same NMR, and hence conformational, parameters in both solvents.

The vicinal scalar coupling constants were used, via a novel approach to five-membered rings, to assign *pro-R* and *pro-S* protons, to give unique values of χ^1, χ^2, and χ^3, and to propose that the prolyl ring conformation in Me_2SO-d_6 and CD_3OD is the same as that found in many crystalline peptides containing prolyl residues, viz., the Ramachandran B conformation (Ramachandran et al., 1970).

Confirmation (see later) of *pro-R* and *pro-S* assignments by the above method was obtained by using a complementary technique, viz., proton–chromophore distance measurement from anomalous chemical shifts.

(*1*) *Spin–Spin Analysis.* The procedure for prolyl spectral analysis was as follows. (a) The DSD spectrum (Figure 6) obtained by irradiation of H^α proved that the H^α, $H^{\beta D}$, and $H^{\beta U}$ spin system was first order since $\Delta_{\beta\beta}$, the chemical shift difference, was 85 Hz. Thus, irradiation at each of the $H^{\beta D}$ and $H^{\beta U}$ resonances collapsed the H^α multiplet to doublets from which $^3J_{\alpha\beta D}$ and $^3J_{\alpha\beta U}$ were obtained by inspection and then by simulation. (b) Irradiation of the isolated $H^{\delta D}$ multiplet gave DSD multiplets (Figure 6F′) corresponding to $H^{\delta U}$, $H^{\gamma D}$ and $H^{\gamma U}$. Accurate chemical shifts of $H^{\delta U}$ and $H^{\gamma U}$ were thus obtained but, due to the small $^3J_{\delta U\gamma D}$, and also overlap of $H^{\gamma D}$ and the methyl resonances of tyrocidine A, accurate $H^{\gamma D}$ chemical shifts were not obtained in this ex-

periment. (c) Irradiation of $H^{\gamma U}$ gave as expected DSD multiplets for $H^{\delta D}$, $H^{\delta U}$, $H^{\beta D}$, $H^{\beta U}$, and $H^{\gamma D}$ (Figure 6E′). In addition, a strong NOE was detected, between $H^{\gamma U}$ and $H^{\gamma D}$, consistent with the close approach of $H^{\gamma D}$ and $H^{\gamma U}$. Thus, from (a)–(c), all prolyl proton chemical shifts were obtained as well as two vicinal coupling constants, $^3J_{\alpha\beta D}$ and $^3J_{\alpha\beta U}$. (d) Triple resonance experiments involving $H^{\gamma D}$ and $H^{\gamma U}$ irradiation gave conventional spectra with doublets at $H^{\delta D}$ and $H^{\delta U}$ from which $^2J_{\delta\delta}$ was obtained by inspection. The value was in good agreement with the $^2J_{\delta\delta}$ value obtained from [[γ,γ-^{2}H]proline]gramicidin S. (e) A similar experiment involving simultaneous irradiation of $H^{\gamma D}$ and $H^{\delta U}$ gave $^3J_{\gamma D\delta D}$ from the collapsed $H^{\delta D}$ multiplet. (f) Because $H^{\beta U}$ and $H^{\gamma D}$ were relatively close (36 Hz), simultaneous irradiation of them plus $H^{\beta D}$ gave a spectrum with collapsed multiplets at $H^{\delta D}$, $H^{\gamma U}$, and $H^{\delta U}$. Under these irradiation conditions, the $H^{\gamma U}$ and $H^{\delta D}$ multiplets were part of an AMX spin system, and, since $^2J_{\delta\delta}$ was known, the approximate values of $^3J_{\gamma U\delta D}$ and $^3J_{\gamma U\delta U}$ were obtained by inspection of the $H^{\gamma U}$ and $H^{\delta D}$ multiplets. (g) Similar triple-resonance experiments in which $H^{\beta U}$, $H^{\gamma D}$, and $H^{\delta U}$ were simultaneously irradiated made H^{α}, $H^{\beta D}$, $H^{\gamma U}$, and $H^{\delta D}$ an AMXY spin system; analysis of its collapsed $H^{\gamma U}$ and $H^{\delta D}$ multiplets gave approximate $^3J_{\gamma U\delta D}$ and $^3J_{\beta D\gamma U}$ values.

At this stage in the prolyl spectral analysis, the only NMR parameters remaining undetermined were $^3J_{\beta D\gamma D}$, $^3J_{\beta U\gamma D}$, $^3J_{\beta U\gamma U}$, $^3J_{\gamma D\delta U}$, $^2J_{\beta\beta}$, and $^2J_{\gamma\gamma}$.

(h) Because of the correspondence between the H^{α}, H^{β}, and H^{δ} parameters of the prolyl residues of tyrocidine A and [[γ,γ-^{2}H]proline]gramicidin S, it was assumed, reasonably, that $^2J_{\beta\beta}$ was the same for their prolyl residues. $^2J_{\gamma\gamma}$ could not be obtained experimentally; it was assumed to be between the values of $^2J_{\beta\beta}$ and $^2J_{\delta\delta}$. (i) The rest of the prolyl vicinal coupling constants were estimated from DSD spectra, from NOEs, and by model building. $^3J_{\beta U\gamma U}$ was estimated to be ca. 9.5 Hz by inspection of the DSD patterns of $H^{\beta U}$ or $H^{\gamma U}$ resonances when $H^{\gamma U}$ or $H^{\beta U}$ was irradiated (parts E′ and C′ of Figure 6). The small NOE between these two protons supported this conclusion. $^3J_{\beta D\gamma D}$ was estimated to be in the range of 1.5 Hz by inspection of the DSD pattern and NOE of $H^{\beta D}$ while irradiating $H^{\gamma D}$ (Figure 6D′). $^3J_{\gamma D\delta U}$ was similarly estimated by inspecting DSD patterns and the medium-size NOEs on each of $H^{\gamma D}$ or $H^{\delta U}$ resonance while the other was irradiated (parts D′ and G′ of Figure 6).

All of the above information was then used to simulate trial DSD (Figure 6) and conventional double- and triple-resonance spectra, until a best fit with the observed DSD spectra was obtained. The errors in various J values varied as seen in Table IV and in Figures 8, 9, 10, and 11.

(2) Double-Karplus/Ring-Closure Approach to Total Conformational Analysis of Prolyl Rings. Although spin–spin analysis yielded all twelve coupling constants and seven chemical shifts of the prolyl residue of tyrocidine A, prolyl conformational analysis was still not straightforward since several questions remained unanswered. These questions, which have not yet been addressed in the literature, include assignment of the *pro-R* and *pro-S* configurations of the six ring protons and unequivocal determination of χ^1, χ^2, χ^3, and χ^4. The double-Karplus/ring-closure approach depicted in Figures 8–11 solved all of these difficulties. The elimination of certain χ^1 values consistent with Karplus curves and observed ^3J values is analogous to the proposal of ϕ,ψ maps and calculations by Gibbons et al. (1970) to reduce degeneracy in $^3J_\phi$ vs. ϕ relationships. In Figures 8–11 χ^i angles forbidden by the fact that they do not allow ring closure are shown by horizontal lines above the Karplus curves for $^3J_\chi$ vs. χ.

Table IV: Conformational and NMR Parameters[a] of the Prolyl Residue in Tyrocidine A. Comparison with Those Predicted for the Ramachandran A and B Conformations[b,c]

dihedral angle[b]	^3J (Hz) A	^3J (Hz) B	^3J (Hz) obsd	obsd χ (deg)
χ^1 H^{α}–$H^{\beta D}$	4.8–9.3	1.7–1.4	1.4 ± 0.5	+30
H^{α}–$H^{\beta U}$	9.8–7.8	8.9–7.8	7.8 ± 0.2	
χ^2 $H^{\beta D}$–$H^{\gamma D}$	6.7–10.7	1.4–1.6	1.5 ± 1.0	−34
$H^{\beta D}$–$H^{\gamma U}$	9.3–6.4	7.8–7.1	7.0 ± 1.0	
$H^{\beta U}$–$H^{\gamma D}$	9.3–6.4	7.8–7.1	7.0 ± 3.0	
$H^{\beta U}$–$H^{\gamma U}$	2.1–1.7	9.3–10.0	9.5 ± 2.0	
χ^3 $H^{\gamma D}$–$H^{\delta D}$	6.7–9.3	1.7–1.5	1.5 ± 1.0	+30
$H^{\gamma D}$–$H^{\delta U}$	9.3–7.8	8.9–7.1	8.0 ± 2.0	
$H^{\gamma U}$–$H^{\delta D}$	9.3–7.8	8.9–7.1	8.0 ± 1.0	
$H^{\gamma U}$–$H^{\delta U}$	2.1–1.4	7.6–10.0	9.5 ± 1.0	

[a] $^2J_{\beta D\beta U} = -12.9$ Hz and $^2J_{\delta D\delta U} = -10.0$ Hz are consistent with the corresponding values in [[γ,δ-^{2}H]proline]gramicidin S (Kuo et al., 1979); $^2J_{\gamma D\gamma U} = -12.0$ Hz is consistent with Figure 6. [b] Ramachandran et al. (1970). The A conformation has $\phi = -70°$ to $-40°$, $\chi^1 = -5°$ to 30°, $\chi^2 = 15°$ to 40°, $\chi^3 = -15°$ to $-30°$, $\chi^4 = 5°$ to 20°; the B conformation has $\phi = -60°$ to 70°, $\chi^1 = 20°$ to 30°, $\chi^2 = -30°$ to 35°, $\chi^3 = 20°$ to 35°, $\chi^4 = -5°$ to 20°. The ^3J values corresponding to A and B are seen in columns 3 and 4 of this table. [c] The stereochemical assignments of the β, γ, and δ protons are given in Figure 9.

The recognition that two Karplus curves govern relationships between a proton and the *pro-R* and *pro-S* protons of a methylene group was published by Bystrov (1976), who proposed the following relationship for the NH–CH_2 of glycyl residues. This was extended to glycyl and cystine methylene groups of oxytocin (Wyssbrod et al., 1977).

Here we combine these two criteria, the double-Karplus (DK) and ring-closure (RC) criteria, to total prolyl residue conformational analysis. It should be obvious that this approach applies to all small-ring compounds. It could also be readily extended to other side chains by using conformational energy maps or calculations. The angles for pyrrolidine rings deviate from the classical staggered angles conventionally used for side-chain conformational analysis. The Karplus curve used here was introduced by Deber et al. (1971) to convert ^3J values to dihedral angles, θ, the angle between the two protons involved in the Karplus curve, $^3J_{CH-CH} = A\cos^2\theta + 1.4$, where $A = 8.5$ for $90° > |\theta| > 0°$ and $A = 10.5$ for $180° > |\theta| > 90°$. It should be noted that the conventional definitions of θ and χ for each of the χ^1, χ^2, and χ^3 bonds of prolyl residues are related.

(a) Determination of χ^1 and the Configurations of β Protons. The procedure used to determine χ^1 is shown in Figure 8A. The two Karplus curves $^3J_{\alpha\beta R}$ vs. $\theta_{\alpha\beta R}$ and $^3J_{\alpha\beta S}$ vs. $\theta_{\alpha\beta S}$ are shown (dotted and full lines, respectively) and are related by the equation (since the α carbon is in the S configuration) $\theta_{H^{\alpha}-H^{\beta}(R)} = \theta_{H^{\alpha}-H^{\beta}(S)} - 120°$. The torsional angle χ^1, defined by the orientation of the prolyl N and C^{γ} atoms, is related to $\chi^1 = \theta_{H^{\alpha}-H^{\beta}(S)} = \theta_{N-C^{\gamma}}$. When the N and C^{γ} atoms of the prolyl ring are eclipsed, $\chi^1 = 0°$ and H^{α} and $H^{\beta}(S)$ are eclipsed.

Although the spin–spin analysis yielded $^3J_{\alpha\beta U} = 7.8$ Hz and $^3J_{\alpha\beta D} = 1.4$ Hz, it is not known whether $H^{\beta U} = H(S)$ or $H(R)$. In Figure 8A it is assumed that $H^{\beta U}$ is *pro-R* and $H^{\beta U}$ is *pro-S*, and both the values of $^3J_{\alpha\beta}$ are drawn as dotted horizontal lines. The intersections of the latter with their appropriate Karplus curve are designated (□); the large ^3J gives four intersections ($\chi^1 = -140°$, $-30°$, $+30°$, and $+140°$) whereas the small ^3J yields only two intersections ($\chi^1 = -140°$ and $+30°$). Obviously, only $\chi^1 = -140°$ or $+30°$ corresponds to both ^3J values, thus eliminating $\chi^1 = +140°$ and $-30°$.

To distinguish whether $-140°$ or $+30°$ is the correct χ^1 angle, we used the RC criterion. As can be seen in Figure 8A,

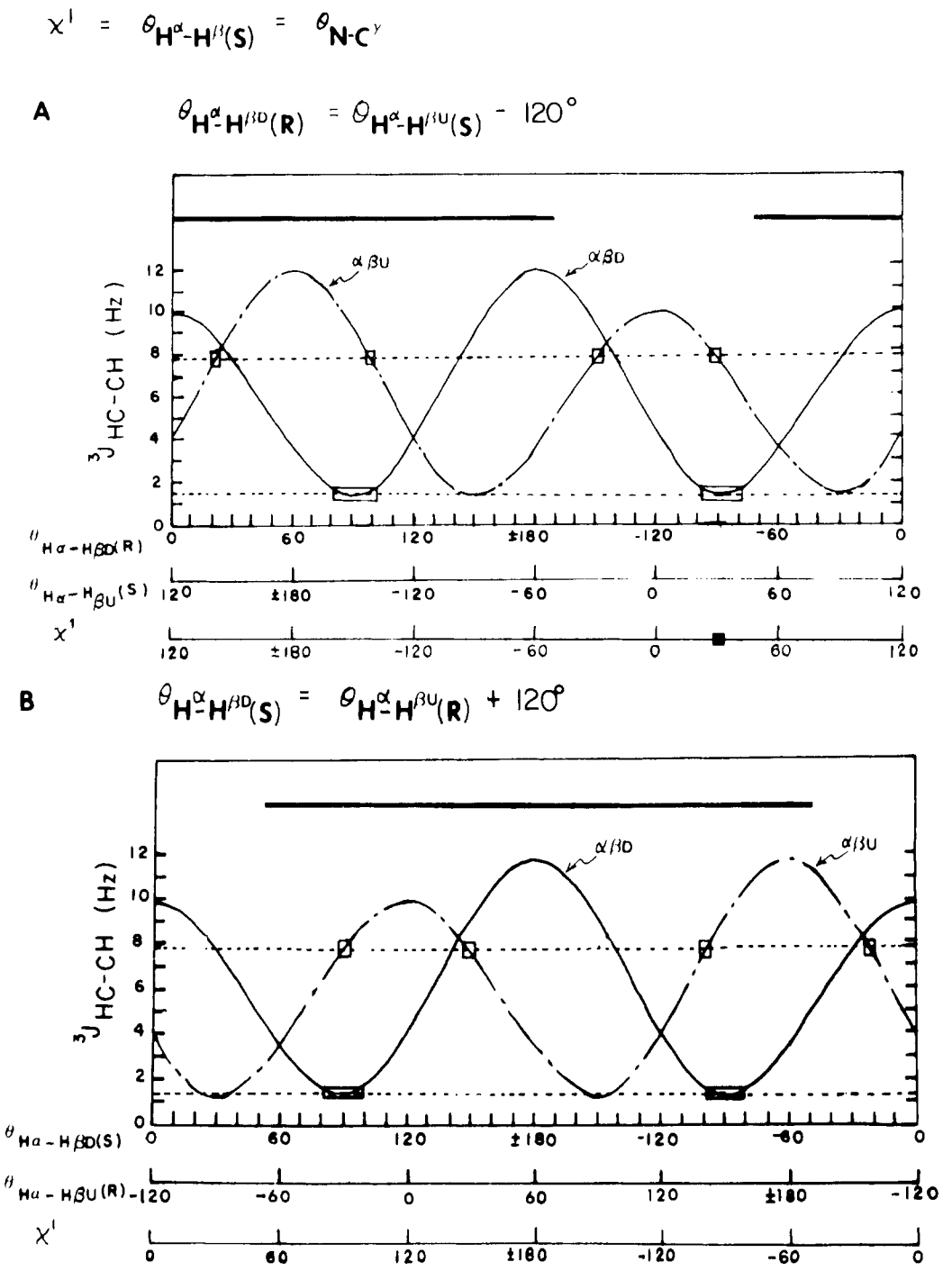

FIGURE 8: Karplus curves for the H^{α}–H^{β} coupling constants, ^3J vs. χ^1, for Pro^5 residue. (A) Assumes $H^{\beta D}$ is *pro-R* and $H^{\beta U}$ is *pro-S*. (B) Assumes $H^{\beta D}$ is *pro-S* and $H^{\beta U}$ is *pro-R*. The heavy solid lines above the Karplus curves correspond to those χ^1 angles which do not allow ring closure (Ramachandran et al., 1970). The open rectangle on the Karplus curve indicates the error of experimental coupling constants; the filled rectangle indicates the range of χ^1 angle deduced to be correct by this procedure.

$\chi^1 = -140°$ is not consistent with ring closure and is thus eliminated as a possible angle.

One further conclusion is possible from Figure 8A; since $^3J_{\alpha\beta D}$ has the extreme value of 1.4 Hz, it is highly unlikely that χ^1 torsional motion occurs. The alternative interpretation is that χ^1 motion is between conformations whose dihedral angles all correspond to extremely low ^3J values.

The assumption that $H^{\beta U} = H(R)$ and $H^{\beta D} = H(S)$ in Figure 8A need not necessarily be true, and to prove or disprove this we drew Figure 8B assuming $H^{\beta U} = H(S)$ and $H^{\beta D} = H(R)$. Applying both the DK and RC criteria to Figure 8B in a manner entirely analogous to that in Figure 8A leads to the conclusion that no χ^1 angle corresponds to both ^3J values. This conclusion is untenable and therefore $H^{\beta U}$ and $H^{\beta D}$ must be the *pro-R* and *pro-S* protons and $\chi^1 = +30°$, as denoted by (■) in Figure 8A.

(*b*) *Determination of* χ^2 *and* γ*-Proton Configurations.* (1) Because there are two β and two γ protons, four Karplus curves were drawn assuming $H^{\gamma D} = H(R)$ and $H^{\gamma U} = H(S)$. These are shown in parts A and B of Figure 9, and using the DK plus the RC criteria for the χ^2 angle (namely, χ^2 can only have the values $+50° > \chi^2 > -50°$), it was possible to conclude from Figure 9A and again from Figure 9B that $\chi^2 = -34°$. The Karplus relationships and nomenclature used in Figure 9A,B are given by the following: $\chi^2 = \theta_{H^{\beta D}(R)\text{-}H^{\gamma}(S)} = \theta_{C^{\alpha}\text{-}C^{\delta}}$ and $\theta_{H^{\beta D}(R)\text{-}H^{\gamma D}(R)} = \theta_{H^{\beta D}(R)\text{-}H^{\gamma U}(S)} + 120°$. When $\chi^2 = 0°$ (C^{α}

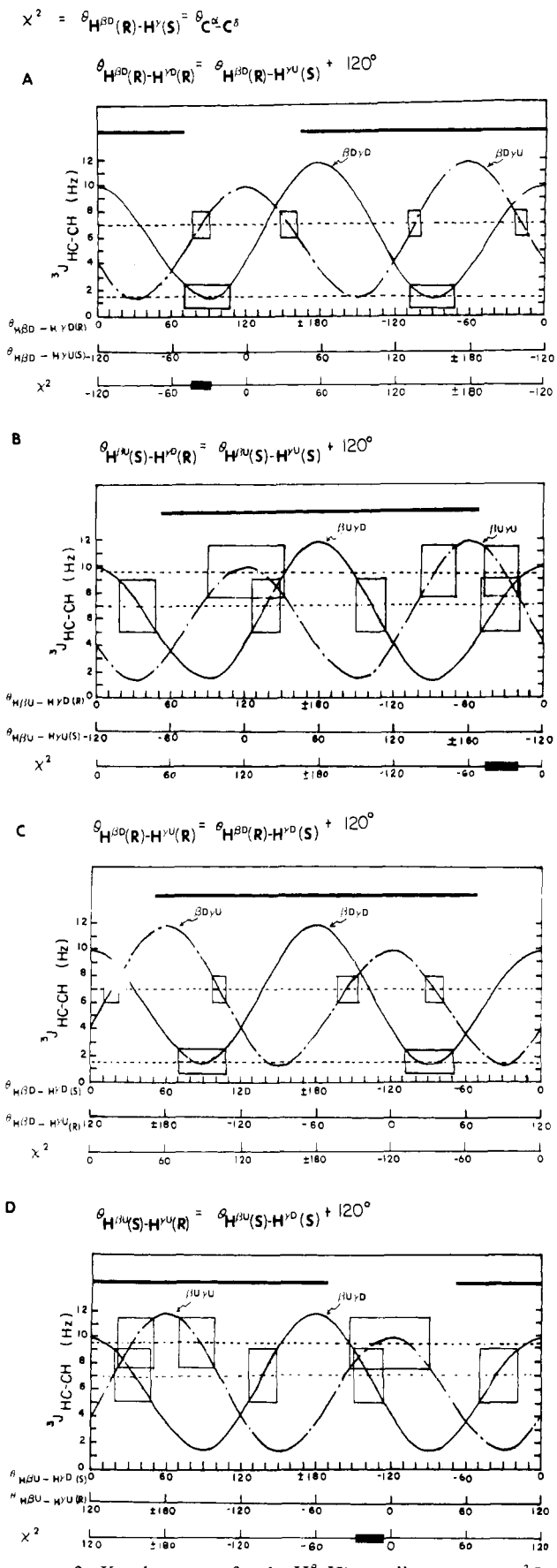

FIGURE 9: Karplus curves for the H^{β}–H^{γ} coupling constants, ^3J vs. χ^2, for possible assignments of γ protons in the Pro^5 residue. The $H^{\beta D}$ and $H^{\beta U}$ are assigned as *pro-R* and *pro-S* (see Figure 8). (A) and (B) assume $H^{\gamma D}$ and $H^{\gamma U}$ are *pro-R* and *pro-S*, respectively. (C) and (D) assume $H^{\gamma D}$ and $H^{\gamma U}$ are *pro-S* and *pro-R*, respectively. The other designations are as described in Figure 8.

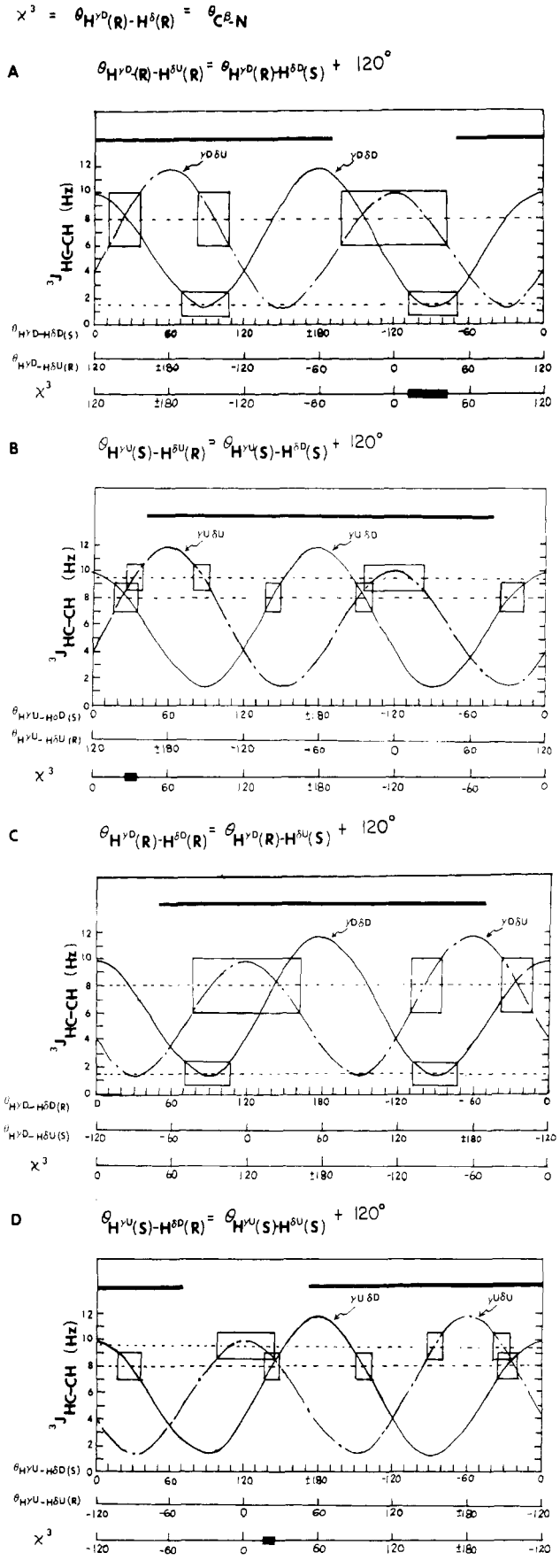

FIGURE 10: Karplus curves for the H^{γ}–H^{δ} coupling constants, ^3J vs. χ^3, for possible assignments of δ protons in the Pro^5 residue. $H^{\gamma D}$ and $H^{\gamma U}$ are assigned as *pro-R* and *pro-S*, respectively (see Figure 9). (A) and (B) assume the $H^{\delta D}$ and $H^{\delta U}$ are *pro-S* and *pro-R*, respectively; (C) and (D) assume $H^{\delta D}$ and $H^{\delta U}$ are *pro-R* and *pro-S*, respectively. The other designations are as described in Figure 8.

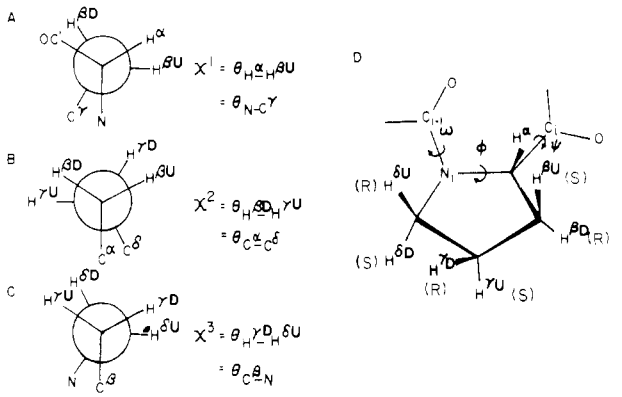

FIGURE 11: (A–C) are Newman projections of the conformation around the C^{α}–C^{β} (A), C^{β}–C^{γ} (B), and C^{γ}–C^{δ} (C) bonds of the Pro^5 residue in tyrocidine A. The torsional angles $\chi^1 = +30°$, $\chi^2 = -34°$, and $\chi^3 = +30°$ are based on Figures 8, 9, and 10, respectively. (D) Schematic of the Ramachandran B conformation of the Pro^5 residue in tyrocidine A. More specifically, this is the C_2–C^{β}_{exo}–C^{γ}_{endo} ring conformer. The *R* and *S* assignments of all CH_2 groups of Pro^5 are shown.

and C^{δ} eclipsed), then the pairs of protons $H^{\gamma U}$ and $H^{\delta D}$ and $H^{\gamma D}$ and $H^{\beta U}$ are eclipsed. (2) As with χ^1/H^{β} determinations, confirmation of the values of χ^2 and the γ-proton *pro-R* and *pro-S* assignments deduced from Figure 9A,B was obtained by examining Figure 9C,D where the opposite assumptions, $H^{\gamma U} = H(S)$ and $H^{\gamma D} = H(R)$, were utilized. Figure 9C predicted no χ^2 angle consistent with the DK and RC criteria whereas Figure 9D yielded $\chi^2 = -20°$. These two conflicting results proved that $H^{\gamma D} \neq H(S)$ and $H^{\gamma U} \neq H(R)$. In Figure 9C,D the two Karplus curves were related by the equations

$$\theta_{H^{\beta D}(R)\text{-}H^{\gamma U}(R)} = \theta_{H^{\beta D}(R)\text{-}H^{\gamma D}(S)} + 120°$$

$$\theta_{H^{\beta U}(S)\text{-}H^{\gamma U}(R)} = \theta_{H^{\beta U}(S)\text{-}H^{\gamma D}(S)} + 120°$$

(*c*) *Determination of* χ^3 *and* δ*-Proton Configurations.* Based upon the C^{α} configuration, the *pro-R* and *pro-S* configurations of H^{β}'s were obtained and the latter utilized to yield the absolute H^{γ} configurations. Procedures entirely analogous to those used for these H^{γ} assignments yielded H^{δ} *pro-R* and *pro-S* assignments. The four Karplus curves of Figure 10A,B yield $\chi^3 = +30°$ whereas the curves of parts C and D of Figure 10 yield χ^3 = no angle and $\chi^3 = +30°$, respectively. Thus, $\chi^3 = +30°$ and the assumption behind parts A and B of Figure 10 must therefore be correct, viz., $H^{\delta U} = H(R)$ and $H^{\delta D} = H(S)$ and $\chi^3 = +30°$. The nomenclature behind Figure 10 is governed by the equations

$$\chi^3 = \theta_{H^{\gamma D}(R)\text{-}H^{\delta}(R)} = \theta_{C^{\beta}\text{-}N}$$

$$\theta_{H^{\gamma D}(R)\text{-}H^{\delta U}(R)} = \theta_{H^{\gamma D}(R)\text{-}H^{\delta D}(S)} + 120°$$

$$\theta_{H^{\gamma U}(S)\text{-}H^{\delta U}(R)} = \theta_{H^{\gamma U}(S)\text{-}H^{\delta D}(S)} + 120°$$

The Karplus curves for parts C and D of Figure 10 are given by the equations

$$\theta_{H^{\gamma D}(R)\text{-}H^{\delta D}(R)} = \theta_{H^{\gamma D}(R)\text{-}H^{\delta U}(S)} + 120°$$

$$\theta_{H^{\gamma U}(S)\text{-}H^{\delta D}(R)} = \theta_{H^{\gamma U}(S)\text{-}H^{\delta U}(S)} + 120°$$

The Newman projections for χ^1, χ^2, and χ^3 deduced from the double-Karplus/ring-closure approach are shown in parts A, B, and C of Figure 11, respectively, along with the relationships between χ angles and θ angles. A diagrammatic representation of the conformation of the prolyl ring is shown in Figure 11D. Despite the large error in several ^3J values for the prolyl ring protons, the data collectively demonstrate

Table V: Comparison of Selected Abnormal Chemical Shifts of Tyrocidine A with Those of Gramicidin S[a] and Corresponding Tetrapeptide Values[b] in Me_2SO-d_6

	chemical shift (ppm)		$\Delta\delta = \delta_{GS} - \delta_{TA}$ (ppm)[e]
	δ_{TA}	δ_{GS}	
$Orn^2 H^{\alpha}$	5.26	4.73	−0.53
D-$Phe^7 H^{\alpha}$	5.55	4.73[c]	−0.82
$Pro^5 H^{\beta D}$	1.42	1.92	+0.50
$Pro^5 H^{\beta U}$	1.11	1.45	+0.34
$Pro^5 H^{\gamma D}$	0.97	1.50	+0.53
$Pro^5 H^{\gamma U}$	0.33	1.50	+1.17
$Pro^5 H^{\delta D}$	3.26	3.56	+0.30
$Pro^5 H^{\delta U}$	2.13	3.56[d]	+1.43
$Phe^6 H^{\beta D}$	2.21	3.07[b]	+0.86
$Phe^6 H^{\beta U}$	2.17	2.79[b]	+0.63

[a] M. Kuo (unpublished data in Me_2SO-d_6). [b] Bundi et al. (1975). They did not evaluate proline or ornithine chemical shifts in Me_2SO-d_6. [c] Phe^6-D-Phe^7-Asn^8-Gln^9-Tyr^{10} in tyrocidine A corresponds to Val^6-Orn^7-Leu^8-D-Phe^9-Pro^{10} in gramicidin S, respectively. This enables us to find the additional chemical shift contribution from the Phe^6 and D-Phe^7 rings of tyrocidine A. [d] We assumed the chemical shift of $Pro^5 H^{\delta D}$ in gramicidin S as the normal chemical shift because it has very little, if any, ring-current shifts from that of D-Phe^4. [e] $\Delta\delta = \delta_{GS} - \delta_{TA}$ represents the measured chemical shift anisotropy due to ring-current effect of all aromatic residues in tyrocidine A.

a unique conformation for the prolyl residue. Part of the reason for this statement lies in the value of $^3J_{\alpha\beta D} = 1.4$ Hz. Taken alone, this exceedingly small coupling constant is best interpreted in terms of one χ^1 prolyl angle; however, since all three χ angles are exceedingly close to Ramachandran B conformation (Table IV) commonly found in crystalline peptides, it is not unreasonable to propose within experimental error that only one prolyl conformation exists for tyrocidine A in solution.

Chemical Shift–Conformation Correlations. Proton–Chromophore Distances. Chemical shifts are not generally used for studying conformation or dynamics of peptides, although there are notable exceptions (Kopple & Ohnishi, 1969; Ohnishi & Urry, 1969; Urry et al., 1974). Since the solution conformations of tyrocidine A and gramicidin S are now well established at the ϕ,ψ and χ^1 levels, they can be used to explore or establish conformation–chemical shift relationships or to provide additional conformational details not readily available from the latter parameters, e.g., χ^2 determination. Chemical shift data can also prove that the secondary and tertiary conformations established by scalar coupling constants and proton relaxation parameters are correct.

Conformational information can be extracted either because the shifts are "normal" or because the protons are removed from their "normal" position—usually by diamagnetic anisotropy. Sixteen chromophoric groups with strong diagmagnetic anisotropy exist in tyrocidine A: four aromatic rings, ten backbone peptide linkages, and two carboxamides.

Two definitions of normal chemical shifts can be utilized. Bundi et al. (1975) have evaluated the chemical shifts of X residues in the sequence F_3Ac-Gly-Gly-L-X-L-Ala-OCH_3; X stands for one of the 20 common amino acids. While not perfect examples of random-coil conformations, their data are still intrinsically useful. Comparison of the chemical shifts of the corresponding residues of gramicidin S (Jones et al. 1977, 1978a, 1979; Kuo et al., 1979) and tyrocidine A (Table V) also leads to interesting conclusions. In the following treatment we will emphasize the comparison of corresponding proton chemical shifts in gramicidin S and tyrocidine A, since they are almost identical in secondary conformations and have a common pentapeptide sequence but have different aromatic

Table VI: Johnson-Bovey Parameters, ρ and z(Å), for Individual χ^2 Rotamers of the Phenylalanine Residues in Tyrocidine A

	parameters (Å)											
	D-phenylalanine[4]				phenylalanine[6]				D-phenylalanine[7]			
	$\chi^2 = 180°$		$\chi^2 = 90°$		$\chi^2 = 180°$		$\chi^2 = 90°$		$\chi^2 = 180°$		$\chi^2 = 90°$	
	ρ	z	ρ	z	ρ	z	ρ	z	ρ	z	ρ	z
$Pro^5H^{\beta D}(R)$	5.3	1.0	5.1	2.0	7.5	3.6	3.8	7.0				
$Pro^5H^{\beta U}(S)$	3.7	1.1	3.4	1.4	10.5	5.8	7.5	8.0				
$Pro^5H^{\gamma D}(R)$	3.8	0.9	4.1	1.2	6.9	7.0	10.0	4.0				
$Pro^5H^{\gamma U}(S)$	5.3	1.0	5.8	1.3	3.0	3.1	6.0	2.5				
$Pro^5H^{\delta D}(S)$	4.2	1.0	3.8	2.3	2.5	7.5	12.0	3.5				
$Pro^5H^{\delta U}(R)$	2.5	1.6	2.5	1.2	3.7	10.0	1.0	8.2				
D-Phe^7H^{α}									7.5	1.8	6.0	4.4
Orn^2H^{α}									9.0	6.0	9.0	5.0
$Phe^6H^{\beta D}$									5.5	4.8	4.5	6.6
$Phe^6H^{\beta U}$									4.5	7.0	6.5	4.0

[a] D-Phe[4], Phe[6], and D-Phe[7] have principal χ^1 values from Table III. [b] Pro[5] has $\phi,\psi = -70°,0°$ and a Ramachandran B conformation (Kuo, 1979). [c] Orn[2], Phe[6], and D-Phe[7] are in the antiparallel β pleated sheet conformation.

Table VII: Comparison of Predicted and Observed Anomalous Chemical Shifts from Ring-Current Anisotropy

	chemical shifts							
	D-phenylalanine[4]			phenylalanine[6]		D-phenylalanine[7]		
	$\Delta\delta(180°)^a$	$\Delta\delta(90°)^a$	$\Delta\delta$(obsd)^{b,c}	$\Delta\delta(180°)^a$	$\Delta\delta(90°)^a$	$\Delta\delta(180°)^a$	$\Delta\delta(90°)^a$	$\Delta\delta$(obsd)^b
$Pro^5H^{\beta D}(R)$	-0.0_6	+0.0	+0.50	-0.0_3	+0.2			
$Pro^5H^{\beta U}(S)$	-0.1_5	+0.2	+0.34	0.0	$+0.0_5$			
$Pro^5H^{\gamma D}(R)$	-0.1_5	+0.2	+0.53	$+0.0_5$	0.0			
$Pro^5H^{\gamma U}(S)$	-0.0_6	+0.1	+1.17	+1.0	−0.2			
$Pro^5H^{\delta D}(S)$	−0.1	+0.1	+0.3	+0.2	-0.0_5			
$Pro^5H^{\delta U}(R)$	−0.3	+1.0	+1.43	+0.2	+0.3			
D-Phe^7H^{α}						−0.2	0.0	−0.82
Orn^2H^{α}						0.0	0.0	−0.53
$Phe^6H^{\beta D}$						+0.1	+0.2	+0.63
$Phe^6H^{\beta U}$						+0.2	0.0	+0.86

[a] The columns are the chemical shift anisotropies calculated from the corresponding ρ,z values of Table VI. [b] $\Delta\delta$(obsd) are the observed chemical shifts calculated from the observed values in Table V. [c] The sum of the effects of D-Phe[4] and Phe[6] must be included.

residues at positions 6, 7, and 10 in the sequence. D-Phe[4] ring-current effects are the same in tyrocidine A and gramicidin S, but additional features arising from ring currents of residues 6 and 7 are readily explained.

Certain assumptions were required in order to calculate anomalous chemical shifts: (1) the ϕ,ψ angles and the principal χ^1 rotamer were known for the aromatic residue and the residue containing the anomalously shifted proton, (2) the Johnson–Bovey diagrams (Johnson & Bovey, 1958) were used to calculate anomalous shifts from ρ,z values, (3) two ρ and z values were calculated for each anomalously shifted proton from the Kendrew tyrocidine A model (Kuo, 1979), one ρ,z pair corresponding to $\chi^2 = 180°$ aromatic configuration and one for the $\chi^2 = 90°$. These assumptions can all be questioned but only first-order effects were calculated; e.g., we ignored the effect of χ^1 rotamer equilibria for the aromatic residue and assumed that χ^1 and χ^2 only had the classical configurations found predominantly in crystals.

The effects of D-Phe[4] on the protons of Pro[5] were assumed to be the same in both tyrocidine A and gramicidin S (all δ and J values support this strongly), and the first part of Table VI shows the ρ,z pairs calculated for the $\chi^2 = 180°$ and $\chi^2 = 90°$ rotamers when χ^1 was assumed fixed in the 180° rotamer. Table VII contains the calculated and the observed shifts. Although great accuracy is not claimed, the data for $Pro^5H^{\delta D}$ and $H^{\delta U}$ clearly favor the hypothesis that D-Phe[4] predominantly occupies the $\chi^1,\chi^2 = 180°,90°$ conformation. This holds true for both tyrocidine A and gramicidin S.

Model building, assuming the βII′ turn, as well as our calculations does not fully account for the prolyl β or γ chemical shifts in tyrocidine A. In order to account for the huge, +1.27-ppm shift of $Pro^5H^{\gamma}(S)$ with respect to its shift in gramicidin S (which has no aromatic residue in position 6), we calculated all ρ,z pairs and, hence, ring-current shifts due to the $\chi^2 = 180°$ or 90° conformations of Phe[6] assuming that $\chi^1 = -60°$ for Phe[6]; a clear preference for $\chi^2 = 180°$ rather than 90° for the Phe[6] was found.

For tyrocidine A the agreement is excellent considering the approximations involved, and if one sums up the effects of both D-Phe[4] and Phe[6] for the γ and δ protons, the agreement improves (see Table VII).

Using models, one can predict that D-Phe[7] should exert ring-current effects in either the $\chi^1,\chi^2 = +60°,180°$ or the $+60°,+90°$ conformations. In fact, experimentally large anomalous shifts were observed for D-Phe^7H^{α}, Orn^2H^{α}, and both Phe^6H^{β}'s. However, calculated ρ,z values for D-Phe[7] were not (Tables VI and VII) in quantitative agreement with the observed shifts for these protons. We attribute this disagreement to nonclassical χ^2 and/or χ^1 conformers of D-Phe[7], but further experiments and calculations are needed. It was true, however, that $\chi^2 = 150°$ for D-Phe[7] predicted the directions but not the full magnitudes of the D-Phe^7H^{α}, Orn^2H^{α}, and Phe^6H^{β}'s anomalous shifts.

Pro-R and Pro-S Proton Assignments. Unless *pro-R* and *pro-S* β protons are assigned, spin–spin analysis of proton multiplets does not distinguish $\chi^1 = 180°$ from $\chi^1 = -60°$ rotamers in L amino acids. This difficulty has been surmounted in the past by utilizing heteronuclear coupling constants (Hansen et al., 1975, 1977) and chemical shifts (Dygert et al., 1975; Jones et al., 1979). Appeal to conformational

energy maps or, better, calculations can resolve the problem but some uncertainty remains. Another approach, asymmetric synthesis with ^2H isotopes, can be used. Apart from the use of chemical shifts, these methods are time consuming and often expensive.

Under Conformation Analysis and *Pro-R* and *Pro-S* Assignments of the Prolyl Residue from Spin–Spin Analysis, we demonstrated that for five-membered rings *pro-R* and *pro-S* assignments could be deduced from ^3J values.

Here we demonstrate that a combination of DSB and NOEDS and/or chemical shifts can also assign *pro-R* and *pro-S* protons.

Asn^8 *Pro-R and Pro-S Protons.* The predominant, if not exclusive, conformation of Asn^8, $\chi^1 = +60°$, has both β protons gauche to the α proton. *Pro-R* and *pro-S* β-proton assignments were possible because the Gln^{9}NH gave a differential NOE to each gauche β proton of Asn^8. On the basis of the interproton distance between the amide and α proton of Gln^9, with the NOE ratio method (Jones et al., 1978b–d, 1979; Kuo et al., 1978), the distances between Gln^{9}NH and the βD and βU protons of Asn^8 were calculated to be 2.1 and 3.2 Å, respectively. These distances are also consistent with the NOEs between the α proton of Asn^8 and each of Asn$^8H^{\beta D}$, Asn$^8H^{\beta U}$, and Gln^{9}NH. The low-field, βD proton of Asn^8 is therefore the *pro-S* proton; the βU proton is the *pro-R* proton.

D-*Phe*^{4} *Pro-R and Pro-S Protons.* The *pro-R* and *pro-S* proton assignments of D-Phe^4 were based on the fact that in the $\chi^1 = 180°$ and $\chi^2 = 90°$ conformation, Pro$^5H^{\delta U}$ was anomalously shifted. That the $H^{\delta U}$ moves to lower field with increasing temperature (decreasing $\chi^1 = 180°$ rotamer population) supported this assignment (Dygert et al., 1975; Jones et al., 1979). Unequivocal proof that βD and βU are the *S* and *R* protons, respectively, came from magnitudes of the observed χ^1 NOEs between the NH or $C^\alpha H$ protons of D-Phe^4 and its two β protons, as in the Asn$^8H^\beta$ assignments from the Gln^{9}NH assignments. Thus, the D-Phe^4(NH $\rightarrow$ βD) and D-Phe^4(NH $\rightarrow$ βU) NOEs were 7 and 5%, respectively.

Phe^6 *and* D-*Phe*^{7} *Pro-R and Pro-S Protons.* Assignment of the configuration of the β protons of these two residues was based upon the anomalous chemical shift of the γ protons of Pro^5, the α protons of D-Phe^7 and Orn^2, and the β protons of Phe^6. Confirmation of the D-Phe^6 assignments came from temperature studies of the anomalously shifted Pro$^5H^{\gamma U}$ (0.33 ppm) relative to Pro$^5H^{\gamma D}$ (0.97 ppm). For example, in the case of D-Phe^7, $^3J_{\alpha\beta}$ values were consistent with one predominant (>85%) trans–gauche rotamer either $\chi^1 = +60°$ or 180°; the $\chi^1 = +180°$ rotamer was excluded because it did not permit the ring of the D-Phe^7 residue to anomalously shift the Phe$^6H^\beta$ proton resonances. Thus, the $\chi^1 = +60°$ was established as the preferred rotamer; it accounted for these anomalous shifts as well as the directions of the anomalous Orn^2 and D-Phe^7 α-proton shifts and, hence, gave D-Phe^7 βD and βU assignments. NOE confirmation of these *pro-R* and *pro-S* assignments and $\chi^1 = +60°$ for D-Phe^7 came from the much larger NOE between the low-field carboxamide proton of Asn^8 and the $R\beta$ proton of D-Phe^7. Phe^6 was similarly assigned.

Pro^5 *Pro-R and Pro-S Assignments.* The use of chemical shifts assigned $H^{\delta U}$ as the *R* proton and $H^{\gamma U}$ as an *S* proton; thus, the former must be closer to the D-Phe^4 ring than $H^{\delta D}$ and the latter must be closer to the Phe^6 ring than $H^{\gamma D}$.

Tertiary Conformation and Molecular Topography of Tyrocidine A. Before discussing the tertiary conformations of the whole tyrocidine A molecule, we will compare, on the basis of our data, the conformations of individual side chains in two solvents. The tertiary conformations of tyrocidine A at the χ^1, χ^2, χ^3, and χ^4 levels will then be discussed. All of this information on tertiary and secondary conformation provided detailed information on the solution topography of the tyrocidine A molecule.

Effect of Solvent on Side-Chain Conformations. With minor exceptions, it is quite clear that the normal chemical shifts, anomalous chemical shifts, side-chain scalar coupling constants, and, hence, side-chain conformations are little affected by solvent. The same is also true of chemical shifts, scalar coupling constants, and other determinants of secondary conformation. The following examples illustrate this. (a) The $H^{\gamma D}$, $H^{\gamma U}$, and $H^{\delta U}$ chemical shifts of Pro^5, the H^β chemical shifts of Phe^6, and the H^α chemical shifts of Orn^2 and D-Phe^7 are equally anomalous in both solvents. (b) The order of α-proton chemical shifts is the same in both solvents except for minor movements of Phe$^6H^\alpha$ and Tyr$^{10}H^\alpha$, and only the D-Phe^7 amide-proton chemical shift is significantly out of order in the two solvents. (c) The actual $^3J_{\alpha\beta}$ scalar coupling constants in the two solvents do not deviate by more than 1 Hz; where only $^3J_{\alpha\beta D} + {}^3J_{\alpha\beta U}$ data are available, this conclusion is slightly less secure but nevertheless exceedingly plausible. (d) The side-chain conformations substantially agree, except that all side chains show a slightly greater degree of freedom in Me_2SO-d_6 than CD_3OD. The side chains of Val^1, Orn^2, and Gln^9 exhibited the greatest change—an additional 10–15% averaging.

In another publication (H. R. Wyssbrod, M. Fein, M. Kuo, and W. A. Gibbons, unpublished experiments), the vicinal coupling constants ($^3J_{NH\text{-}C^\alpha H}$), hydrogen–deuterium exchange rates, and the temperature dependence of amide-proton chemical shifts are similar in both solvents, indicating that the secondary conformation is basically the same in both solvents.

The tertiary conformations and molecular topography of tyrocidine A will therefore be discussed with the assumption that the basic secondary and tertiary features are the same to at least a first-order approximation in both solvents.

Tertiary Conformation at the χ^1 *Level.* Multiplication of the statistical weights of all side-chain conformations yields the statistical weights of all *possible* 3° conformations of the whole molecule (Jones et al., 1979) provided there are no interactions among the side chains of different residues. Generally, for steric reasons, not all of the latter will be thermodynamically allowed, and further experimental and/or theoretical work is usually needed to test the reality of these tertiary conformers.

The principle tertiary conformations of tyrocidine A at the χ^1 level contain certain obvious features: each conformation must have $\chi^1 = 180°$ for D-Phe^4, $\chi^1 = 30°$ for Pro^5, $\chi^1 = -60°$ for Phe^6, $\chi^1 = +60°$ for D-Phe^7, $\chi^1 = +60°$ for Asn^8, and $\chi^1 = -60°$ for Tyr^{10}, but several subsets are possible at the χ^1 level, because two statistically significant χ^1 rotamers exist for Val^1, Orn^2, Leu^3, and Gln^9.

Tertiary Structure at the χ^2 *Level.* As previously discussed, the principal χ^2 conformations of residues 4–6, and 8 have been established from experiment, and so for these residues the χ^1,χ^2 populations are well-defined. Theoretical calculations (Lewis et al., 1973) and crystal structures (Benedetti, 1977) have established that there are two principal χ^1,χ^2 populations for the Leu residue, and our χ^1 data are consistent with these. However, we have not yet established which χ^1,χ^2 combinations are correct in tyrocidine A because we do not yet have *pro-R* and *pro-S* assignments for Leu^3, nor have we performed a spin–spin analysis of its β,γ spin systems. The χ^2 conformation of Asn^8 has been shown to be +90° by NOE studies (Kuo & Gibbons, 1979).

Tertiary Structure at the χ^3 and χ^4 Levels. Only in the case of Pro[5] is this information available from our experiments. In fact, Pro[5] occupies the $\chi^3,\chi^4 = 30°,-15°$. The latter corresponds to the C_2–C_{exo}–C_{endo} conformation found in the crystalline state and implies a Pro[5] side chain with little or no χ motions.

Molecular Topography of Tyrocidine A. The existence of such a high percentage of side chains in a distinctly preferred conformation endows tyrocidine A with distinctly different topographical regions, and the relative independence of the backbone NMR parameters and the structure of solvent imply that those regions are independent of solvent. The relevance of those various regions to biological functions remains to be explored. Region 1 is highly hydrophobic and consists of the side chains of Val[1], Leu[3], D-Phe[4], Pro[5], Phe[6], and D-Phe[7]. Region 2 is hydrophilic and consists of the sequence D-Phe[7]NH→D-Phe[7]CO→Asn[8]NH→Asn[8]CONH$_2$→-Gln[9]CONH$_2$→Tyr[10]OH. The topographical surface formed from these hydrophilic groups is helical. Region 3 is flat and consists of the peptide groups of most amino acid residues in equatorial configurations. The carbonyl peptide groups of D-Phe[4] and Gln[9] and the Orn[2] side chains are axial to this flat molecular plane. The side-chain conformations and the tertiary conformations of tyrocidine A and these topographical regions are entirely consistent with, and support, the proposed secondary structure—a βI turn, a βII′ turn, and an approximate antiparallel β-pleated sheet.

Acknowledgments

We are greatly indebted to Dr. H. R. Wyssbrod for his immensely thorough review of the original form of this paper.

References

Benedetti, E. (1977) in *Peptides: Proceedings of the Fifth American Peptide Symposium* (Goodman, M., & Meienhofer, J., Eds.) pp 257–273, Wiley, New York.

Beyer, C. F., Craig, L. C., & Gibbons, W. A. (1972) *Biochemistry 11*, 4920.

Bundi, A., Grathwohl, C., Hochmann, J., Keller, R. M., Wagner, G., & Wüthrich, K. (1975) *J. Magn. Reson. 18*, 191.

Bystrov, V. F. (1976) *Prog. Nucl. Magn. Reson. Spectrosc. 10*, 41.

Deber, C. M., Torchia, D. A., & Blout, E. R. (1971) *J. Am. Chem. Soc. 93*, 4893.

Dygert, M., Go, N., & Scheraga, H. A. (1975) *Macromolecules 8*, 750.

Fein, M. (1975) Ph.D. Thesis, The City University of New York.

Gibbons, W. A., Nemethy, G., Stern, A., & Craig, L. C. (1970) *Proc. Natl. Acad. Sci. U.S.A. 67*, 239.

Gibbons, W. A., Beyer, C. F., Dadok, J., Sprecher, R. F., & Wyssbrod, H. R. (1975a) *Biochemistry 14*, 420–429.

Gibbons, W. A., Crepaux, D., Delayre, J., Dunand, J. J., Hajdukovic, G., & Wyssbrod, H. R. (1975b) in *Peptides: Chemistry, Structure and Biology* (Walter, R., & Meienhofer, J., Eds.) pp 127–137, Ann Arbor Science Publishers, Ann Arbor, MI.

Hansen, P. E., Feeney, J., & Roberts, G. C. K. (1975) *J. Magn. Reson. 17*, 249.

Hansen, P. E., Batchelor, J. C., & Feeney, J. (1977) *J. Chem. Soc., Perkin Trans. 2*, 50.

Johnson, C. E., Jr., & Bovey, F. A. (1958) *J. Chem. Phys. 29*, 1012.

Jones, C. R., Alper, J. B., Kuo, M., & Gibbons, W. A. (1977) in *Peptides: Proceedings of the Fifth American Peptide Symposium* (Goodman, M., & Meienhofer, J., Eds.) pp 329–332, Wiley, New York.

Jones, C. R., Kuo, M., & Gibbons, W. A. (1978a) *Biomol. Struct. Funct., Symp., 1977*, 401–406.

Jones, C. R., Sikakana, C. T., Hehir, S. P., & Gibbons, W. A. (1978b) *Biochem. Biophys. Res. Commun. 83*, 1380.

Jones, C. R., Sikakana, C. T., Hehir, S. P., Kuo, M., & Gibbons, W. A. (1978c) *Biophys. J. 24*, 815–832.

Jones, C. R., Sikakana, C. T., Kuo, M., & Gibbons, W. A. (1978d) *J. Am. Chem. Soc. 100*, 5960.

Jones, C. R., Kuo, M., & Gibbons, W. A. (1979) *J. Biol. Chem. 254*, 10 307–10 312.

Kopple, K. D., & Ohnishi, M. (1969) *J. Am. Chem. Soc. 91*, 962–970.

Kopple, K. D., Wiley, G. R., & Tauke, R. (1973) *Biopolymers 12*, 627.

Kuo, M. (1979) Ph.D. Thesis, University of Wisconsin, Madison, WI.

Kuo, M., & Gibbons, W. A. (1979) *J. Biol. Chem. 254*, 6278–6287.

Kuo, M., Ford, J. J., & Gibbons, W. A. (1978) *Pept., Proc. Eur. Pept. Symp., 15th*, 1977.

Kuo, M., Jones, C. R., Mahn, T. H., Miller, P. R., Nicholls, L. J. F., Ford, J. J., & Gibbons, W. A. (1979) *J. Biol. Chem. 254*, 10 301–10 306.

Lakshninarayanan, A. V., Sasisekharan, V., & Ramachandran, G. N. (1967) in *Conformation of Biopolymers* (Ramachandran, G. N., Ed.) Vol. I, p 61, Academic Press, New York.

Lee, S. G., Littau, V., & Lipmann, F. (1975) *J. Biol. Chem. 66*, 233.

Lewis, P. N., Momany, F. A., & Scheraga, H. A. (1973) *Isr. J. Chem. 11*, 121.

Ohnishi, M., & Urry, D. W. (1969) *Biochem. Biophys. Res. Commun. 36*, 194–202.

Pachler, K. G. R. (1964) *Spectrochim. Acta 20*, 581–587.

Rae, I. D., & Scheraga, H. A. (1978) *Biochem. Biophys. Res. Commun. 81*, 481.

Ramachandran, G. N., Lakshninarayanan, A. V., Balasubramanian, R., & Tegoni, G. (1970) *Biochim. Biophys. Acta 221*, 165.

Ristow, H. (1977) *Biochim. Biophys. Acta 477*, 177.

Sarkar, N., & Paulus, H. (1972) *Nature (London), New Biol. 239*, 228.

Schröder, E., & Lubke, K. (1966) in *Peptides*, Vol. II, pp 424–444, Academic Press, New York and London.

Urry, D. W., Mitchell, L. W., & Ohnishi, T. (1974) *Biochemistry 13*, 4083–4090.

Wyssbrod, H. R., Fein, M., Dadok, J., Sprecher, R. F., Beyer, C. F., Craig, L. C., Ziegler, P., & Gibbons, W. A. (1973) *Abstracts of Papers*, 166th National Meeting of the American Chemical Society, Chicago, IL, 1973; American Chemical Society, Washington, D.C., 1973, BIOL 184.

Wyssbrod, H. R., Ballardin, A., Schwartz, I. L., Walter, R., Van Binst, G., Gibbons, W. A., Agosta, W. C., Field, F. H., & Cowburn, D. (1977) *J. Am. Chem. Soc. 99*, 5273.